Journal of Metals, Materials and Minerals, 36(1), e2510, 2026

Investigation on the tribological properties of Al_2O_3-TiC substrates in fixed abrasive lapping for data storage applications

Benjie Locsing FERNANDEZ[1,2], Thanakrit SRISUWAN[2], Duangamol TUNGASMITA[3], and Sukkaneste TUNGASMITA[4,*]

[1] *Nanoscience and Technology Program, Graduate School, Chulalongkorn University, Bangkok 10330, Thailand*
[2] *Western Digital Storage Technologies (Thailand) Ltd., Bang Pa-in, Phra Nakhon Si Ayutthaya 13160, Thailand*
[3] *Department of Chemistry, Faculty of Science, Chulalongkorn University, Bangkok 10330, Thailand*
[4] *Department of Physics, Faculty of Science, Chulalongkorn University, Bangkok 10330, Thailand*

***Corresponding author e-mail**: Sukkaneste.t@chula.ac.th

Received date:
24 September 2025
Revised date:
11 December 2025
Accepted date:
17 December 2025

Keywords:
AlTiC substrate;
Fixed abrasive;
Lapping material removal rate;
Coefficient of friction;
Surface finish

Abstract

Alumina titanium-carbide (Al_2O_3-TiC) or simply AlTiC substrates were widely used in the magnetic recording industry for their superior mechanical and tribological properties. This study investigated the effect of AlTiC substrate crystal structure, chemical bonding and grain size in slider fix abrasive lapping tribology. Two types of AlTiC substrates, Type-A AlTiC and Type-B AlTiC equipped with an electro lapping guide (ELG), fully functional reader and writer devices were used in the study. The type-B lower material removal rate resulting to rougher surface finish was mainly due weakening caused by the titanium oxycarbide phase, which was the dominant factor, outweighing the minimal contribution from grain-boundary strengthening (Hall-Petch effect). Furthermore, the grain size investigated in this study was between 420 nm to 670 nm, making it far too large for the inverse Hall–Petch effect which involves softening at exceedingly small grain sizes typically below 100nm to be a relevant mechanism. The findings also highlight the importance of lapping parameters optimization to balance material removal rate (process productivity and efficiency) and surface finish (magnetic head reliability and areal density performance).

1. Introduction

The Magnetic Hard Disk Drive (HDD) remains a cornerstone of modern computing. It functions as a primary storage device by reading and writing magnetic binary bits onto a high-speed spinning disk, known as a platter. The core of HDD performance lies in the read-write head assembly, or slider. The core of HDD performance lies in the read-write head assembly, or slider. This tiny structure "flies" just nanometers above the media platter. During operation, the slider performs two critical functions: it transforms the platter's magnetic field into an electrical signal (data reading) and converts an electrical current into a magnetic field (data writing) to achieve high-speed data access. The structure of slider consists of multilayers of thin film materials, which is well-designed and grown on aluminum oxide and titanium carbide (Al_2O_3-TiC), known for industry as: "AlTiC" substrate. Over the years, the data storage industry has been continuously expanding. As the industry pushes for higher areal density (storage capacity), the physical gap between the head and the media must continue to shrink[1]. Currently, this separation is a mere few nanometers, necessitating absolute control over the surface topography of both the slider and the disk.

The AlTiC is a two-phased composite material consisting of alumina (Al_2O_3) and titanium carbide (TiC). The substrate material is critical as it influences the tribology of the head/disk interface and the manufacturing process of the magnetic head. Alumina forms the continuous ceramic matrix, which is the insulating and load-bearing backbone of the material. It provides high hardness, chemical stability, and excellent electrical insulation and dielectric properties. Titanium Carbide particles are dispersed uniformly throughout the alumina matrix. It is extremely hard and, crucially, electrically conductive. It also contributes significantly to the overall fracture toughness and wear resistance of the composite.

The desired AlTiC grain size and microstructure were achieved by varying the conditions in hot pressing (HP) [2,3] and hot isostatic pressing (HIP) processes [3]. The hot pressing involves applying heat and uniaxial pressure (from a single direction) to a material, typically a powder, placed in a die. The combination of heat and pressure causes the particles to rearrange, deform, and bond together. While HP is effective for producing dense, high-strength AlTiC, the one-directional nature of the force can lead to non-uniform pressure distribution, often resulting in residual porosity (microscopic voids). On the other hands, HIP process applies heat and isostatic pressure (equal pressure from all directions) to a material inside a high-pressure vessel. The pressure is applied using an inert gas, such as argon, which surrounds the part and exerts force evenly on all surfaces. This ensures a more uniform grain outcome. The HIP is often used as a post-processing step for

castings or additively manufactured parts to eliminate internal porosity. The isostatic pressure collapses internal voids and microscopic pores, resulting in improved final density. Because pressure is applied equally from all sides, the final product has a highly uniform microstructure and consistent properties throughout the entire substrate.

Slider lapping processes involves a series of steps critical in achieving topographical and electrical requirements. The final lapping step applies fixed-abrasive lapping technology where material is removed or polished from the surface of a workpiece precisely to give it a good planar surface finish [4-6]. During lapping contact between moving surfaces, a friction force is generated in tribological regime, which allows the material removal mechanism to start.

From a tribology point of view, AlTiC shows regions of high and low friction, which coincides with the alumina phase for the high friction region and the TiC phase for the low friction region [7]. Generally, the lapping removal rate of this material is a complex function and depends on contact geometry, surface asperities, microstructure, grain sizes, fracture toughness, speed, load, temperature, duration, environment, and lubrication [8]. Material removal occurs through a combination of micro-cutting/ploughing and brittle fracture. For ductile materials (metal films), the abrasive particle cuts a small chip or pushes the material aside. For hard, brittle materials (ceramic substrate), the fixed diamond induces cracks that join, leading to the removal of material fragments. Investigation on the coefficient of friction (COF) lubricated AlTiC substrate surface, lubricant type affects the friction regime, and dependency was observed normal force and sliding speed [9].

This study investigates how the grain size, crystal structure, and chemical bonding of AlTiC substrates influence the tribological characteristics of fixed-abrasive lapping. Our objective is to refine the fabrication process to produce defect-free, ultra-smooth surfaces, which are essential for maximizing recording density and drive reliability.

2. Experimental methods

2.1 AlTiC Substrate material

The AlTiC wafer substrates, eight inch in diameter is supplied by Hitachi Metals, Japan. HP and HIP were involved during substrate fabrication. However, the supplier did not provide details of the processing condition and parameters.

2.2 Grain size, crystal structure and chemical bonding characterization

The AlTiC substrates surface were inspected with Carl Zeiss Merlin field emission scanning electron microscope (FE-SEM). The grain size from the SEM micrographs were measured using the Heyn (1904) intercept method [10].

X-ray diffraction (XRD) technique is used to analyze the atomic and molecular structure of AlTIC substrates. Rietveld modeling, a crystallographic refinement method uses a known or proposed crystal structure to create a theoretical diffraction pattern. This calculated pattern is then meticulously adjusted to fit the experimental XRD data.

The electron microprobe analyzer (EMPA) was used for elemental analysis. This electron interaction causes the atoms in the material to emit characteristic X-rays. By analyzing the wavelength and intensity of these X-rays, the instrument can precisely determine the concentration of each element present in a small volume. EMPA is a quantitative analytical tool used to determine the elemental chemical composition of the AlTiC substrates and is used to measure the exact stoichiometry to determine the precise content in the AlTiC substrates.

Multiple AlTiC substrate fresh from supplier and full device fabricated wafers measuring 46 mm in length and 13 mm width were sampled for XRD and EMPA to confirm crystal structure and chemical bonding characteristics.

2.3 Hardness measurement

The material bulk hardness (HV) of both groups of AlTiC substrates were evaluated using Vickers indentation technique [11] with a Mitutoyo-MCK-H2. The wafer substrate sample used was 45 mm × 45 mm shape of 1.2 mm thickness. Samples were polished under the same conditions of time, tooling, and fixtures. There were four indents per sample with a load of about 19.6 N (2 kg), and a dwell time of 10 s.

The micro-hardness evaluation, a Hysitron Tribo-indenter using a Berkovich indenter in 2000 μN load force was applied. The samples were actual row bars with surface conditions post final lapping. Three row bars from each substrate were used with seven sampling points per row bar samples.

2.4 Coefficient of Friction measurement

The coefficient of friction (COF), an in-house developed friction tester tool, shown in Figure 1, was employed to study the COF of both groups of AlTiC substrates. Unlike other commercially available systems like ball on disc, this friction tester system was designed to closely simulate actual HDD row bar specimen as it glides along the surface of the plate with fixed abrasive as in the final lapping process. The friction force is measured by detector situated at left and right ends of the row bar. Weight and plate speed in rpm applied on the workpiece (row bar) can be varied to measure friction force and determine the coefficient of friction. A 350 nm monocrystalline diamond embedded in a Sn (99%)–Bi (1%) (725PD) plate was used in the study. A hydrocarbon oil-based lubricant (CK9G supplied by Saint-Gobain) was used in the experiments. Plate speeds were evaluated from 5 rpm to 90 rpm.

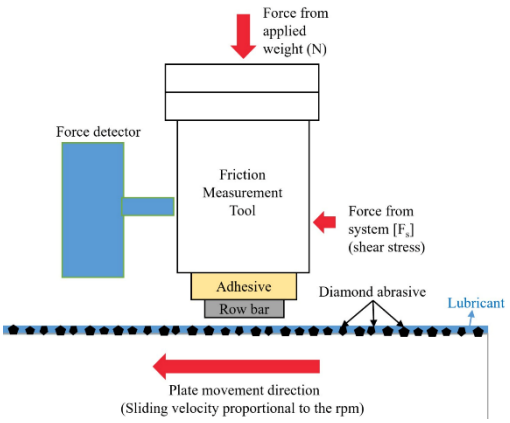

Figure 1. Schematic diagram of the friction tester tool.

The coefficient of friction (COF) [12], or friction coefficient, is a constant defined by

$$\mu = \text{lateral (friction) force normal (F) / externally applied load (N)} \quad (1)$$

$$\mu' = dF/dN \quad (2)$$

In the first Equation (1), F = 0 at N = 0; i.e., the friction force is zero at zero load, while in the second Equation (2), the friction force may be finite at zero load and the COF is given by the slope of the line.

2.5 Lapping material removal rate (LMMR) characterization

Third generation advanced fine lapping (AFL3G) tool was used for the characterization of the lapping performance, i.e., lapping rate. The row bar is attached to the mount tool using a polyurethane adhesive shown in Figure 3(a). Connection from the slider is wire bonded to the PCB shown in Figure 3(b). AFL3G has pogo pins that provides connection to the PCB when the mounted is loaded on the lapping machine. AFL3G is a close loop system and controls lapping process though electrical lapping guides (ELG). The slider is automatically pushed harder against the plate when the resistance is below target and vice versa using force actuators. Fixed abrasive or two-body lapping was employed using an in-bismuth (Sn-Bi) alloy plate textured with a uniform groove and charged with 95 nm diamond abrasive. Lapping force evaluated were from 12 psi to 36 psi per slider and at the plate speed of 5 rpm to 15 rpm. A hydro-carbon oil-based lubricant (CK9G supplied by Saint-Gobain) was used in the experiments. Figure 2 shows the schematic diagram illustrating fixed abrasive lapping.

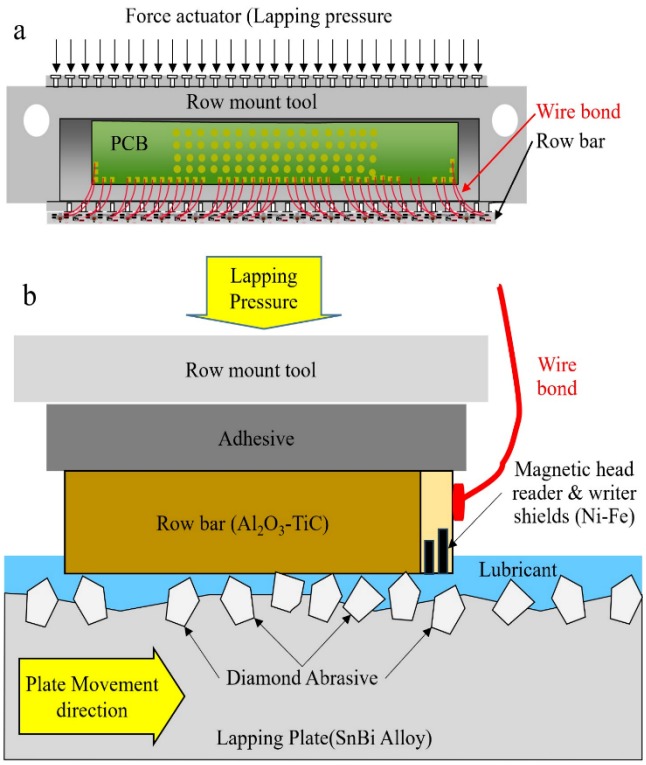

Figure 2. Fixed abrasive lapping schematic diagram. (a) Details of row bar, PCB, wire bond and mount tool, and (b) Plate, abrasive, and row bar on lapping mount too assembly.

2.6 Surface roughness measurement

An atomic force microscope (AFM NX-PTR by Park Systems) was used to investigate the surface roughness of the AlTiC substrate and the Ni-Fe reader shields on HDD slider. The reader shields in a magnetic head are magnetic components that surround the read sensor to precisely define the area from which the sensor can detect magnetic flux. Their primary function is to channel the magnetic flux from the intended data track on a magnetic disk or tape and block stray magnetic fields from adjacent tracks and other sources. AFM scan size of 20 mm × 20 mm and 3.5 mm × 3.5 mm, respectively. Three (3) row bars from each substrate were used with five sampling points per row bar. These row bars underwent normal cleaning procedures after the final lapping process.

3. Results and discussion

3.1 Lapping material removal rate (LMMR), coefficient of friction (COF), hardness, and surface finish

The effect of plate speed and lapping pressure on the lapping material removal rate (LMMR) of magnetic HDD sliders follow the general principles of lapping tribology, as described by Preston's equation [13]. Regarding the material removal rate (MRR) in lapping many researchers rely on the abrasion/wear-based Preston's equation (MRR = K·p·vr), where K is Preston's coefficient, and the predominant input quantities are lapping pressure (p) exerted on the workpiece and the relative speed (vr) from the plate speed. This relationship is critical for achieving the reader and writer element critical dimensions and surface finish needed for optimum performance of magnetic heads for HDD.

The relationship between LMRR and lapping pressure for both type-A and type-B AlTiC substrates is illustrated in Figure 3(a). The value of LMMR increases remarkably with an increasing in the lapping pressure during the process. Thus, the lapping pressure should be optimized within a certain range to ensure optimum magnetic head performance is achieved. It was found that, if the lapping pressure were too high, the lapping diamond abrasive grains were likely to sink faster into the top layer of the lapping plate, LMRR would be reduced quickly. This leads to low performance and productivity in the lapping process of the HDD head. The relationship between LMRR and plate rotation speed is shown in Figure 3(b). With the increase in plate rotation speed, the LMRR increased linearly. For any given lapping pressure and plate speed, it was found that the type-B AlTiC substrate showed higher lapping material removal rate, compared to type-A, as seen in Figure 3(a-b). AlTiC is a brittle material, the fixed diamond induces cracks that join, leading to the removal of material fragments. Titanium Carbide particles are dispersed uniformly throughout the alumina matrix. It is extremely hard and should be the contributing significantly to the overall fracture toughness samples substrates.

The coefficient of friction (COF) values shown in Table 1 indicate that the type-A AlTiC substrate has the COF at 0.21 while that of type-B AlTiC has 0.24 (14% higher than type-A). Higher COF of type-B AlTiC substrate results in a greater shear stress between the

diamond abrasive and the surface of the substrate, resulting a higher LMMR compared to type-A AlTiC substrate. The experimental results demonstrate that the substrate type significantly influences tribological behavior. AlTiC-A consistently provides a lower friction interface compared to AlTiC-B, which is a critical factor for achieving the defect-free, ultra-smooth surfaces required in high-density HDD slider fabrication.

The mechanical characteristics of both type-A and type-B AlTiC substrates are summarized in Table 1. Vicker's hardness of type-A AlTiC substrate is at 2038 HV and is higher with respect to type-B AlTiC substrate at 1791 HV. The results measured from Nano-indentation also confirmed that the type-A AlTiC has a localized hardness higher than type-B AlTiC substrate about 5%. Moreover, the type-A AlTiC substrate is also stiffer, with a Young's Modulus of 316.38 GPa, compared to 305.84 GPa for the type-B AlTiC. The surface nano-indenter penetrated less into type-A AlTiC at contact depth of about 34.4 nm than into type-B AlTiC substrate at 35.7 nm, as shown in Figure 4(a-b).

The Load-Indentation depth curve (also known as a nanoindentation curve) in Figure 4(c), compares the mechanical response of two substrate materials. Hardness and resistance to penetration shows that for any given load, the type-A AlTiC curve reaches a smaller maximum depth than the type-AlTiC curve. Therefore, the type-A AlTiC is harder and more resistant to plastic deformation than type-AlTiC, as it requires less indentation depth to support the same load. In terms of elastic recovery and stiffness, since the final depth is related to the amount of permanent deformation, type-AlTiC appears to exhibit slightly better elastic recovery or less total plastic work compared to the type-A AlTiC.

The RMS surface roughness measured by the AFM shown in Table 1, indicates that at a similar lapping condition or parameter, the type-B AlTiC substrate has higher AlTiC and Ni-Fe reader/writer shield roughness. This implies that higher removal rate from higher COF and lower hardness of the material can cause the diamond to plow with deeper cut through the AlTiC substrate surface resulting in rougher RMS surface roughness.

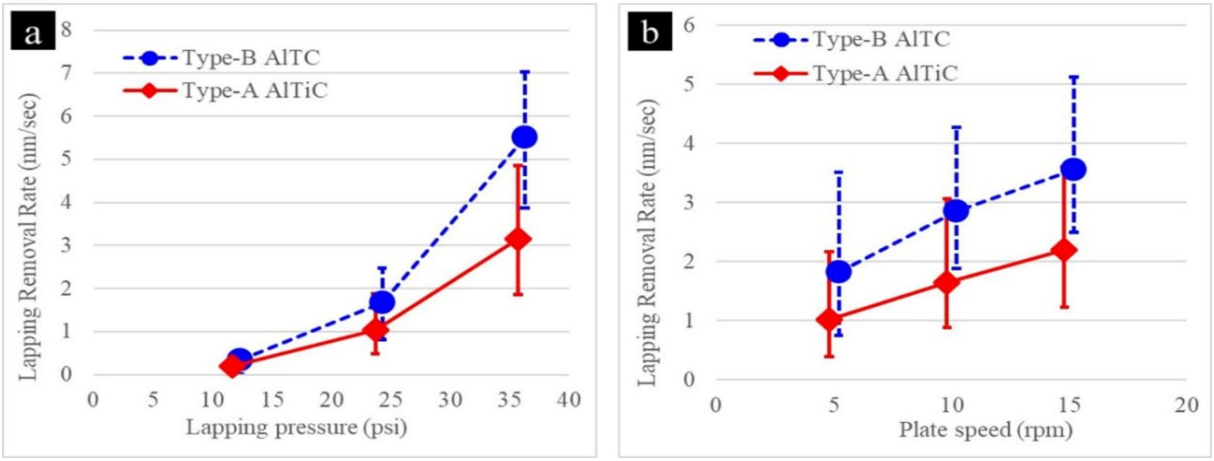

Figure 3. Lapping material removal rate comparison between type-A and type-B AlTiC substrates with respect to (a) lapping pressure, and (b) plate speed.

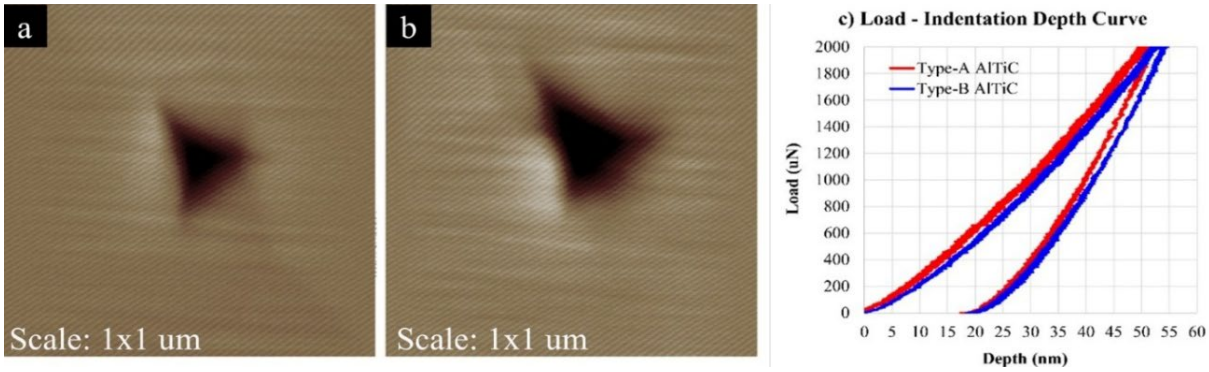

Figure 4. Nano-indentation image (a) type-A AlTiC, (b) type-B AlTiC substrates, and (c) Load -indentation depth curve.

Table 1. Type-A AlTiC and -B coefficient of friction, hardness, and surface finish comparison.

AlTiC Substrate	Coefficient of Friction (COF)	Vickers hardness [HV]	Nano-Indentation			Surface Roughness (Ra)	
			Hardness [GPa]	Modulus of elasticity [GPa]	Contact Depth [nm]	AlTiC [nm]	NiFe [nm]
Type-A	0.21	2038	32.4	316.4	34.4	0.33	0.29
Type-B	0.24	1791	30.7	305.8	35.7	0.41	0.34

3.2 Influence of AlTiC grain size and chemistry on lapping tribology

As seen from Figure 5(a), the type-A AlTiC substrate has the average grain size at about 0.67 µm, while the type-B AlTiC substrate has 0.42 µm. Thus, the modification of AlTiC grain size was achieved by modifying the conditions in hot pressing (HP) and hot isostatic pressing (HIP) [3,14-16]. In metals, the dependence of the displayed strength as a function of grain size has been successfully described by the empirical Hall-Petch and inverse Hall-Petch relationships. Strengthening is induced by dislocation blockage effects, while softening is triggered by dislocation emission from grain boundaries (GBs) and activation of GB deformation mechanisms, such as grain rotation and GB sliding at fine grain sizes [17-19]. In contrast, in ceramics, due to the nature of their chemical bonding, i.e., strong covalent or ionic bonding, and the crystal structure complexity, dislocation nucleation and motion at ambient temperature are significantly restricted. Hence, while Hall-Petch-like behavior has been observed in ceramics, the physically based explanations for the Hall-Petch relationship in metals, e.g., dislocation pile-up, are not directly applicable to justify their mechanical behavior as a function of grain size [20-22].

The TiC crystal structure from Rietveld refinement of the XRD data is shown in Figure 6, along with the EMPA elemental chemical composition of the AlTiC substrates are summarized in Table 2 The structure of TiC in the type-B AlTiC has some percentages of oxygen that are found on the carbon lattice sites [23]. The grain densification of AlTiC [2] during hot pressing occurs primarily at elevated temperatures and under a curtain applied pressure. Significant densification can occur as both high pressure and elevated temperature are applied simultaneously. Thus, the combination of these two factors is what drives the material to deform and consolidate. HP is typically performed in a vacuum or an inert gas atmosphere (such as argon or nitrogen) to prevent unwanted side reactions. However, achieving a completely oxygen-free environment is difficult. The most common source of oxygen comes from the initial raw materials. The starting powders, as TiC, can have thin surface layers of oxides from previous handling or synthesis steps. At the elevated temperatures used in hot pressing (e.g., 1600°C to 1800°C), these oxides can react with the TiC, leading to the substitution of oxygen for carbon in the crystal lattice.

The fact that TiC is a ceramic material with a cubic crystal structure, within TiC lattice, oxygen can replace carbon atoms to form an oxycarbide phase ($TiC_{1-x}O_x$). The substitution of oxygen for carbon in the TiC lattices of AlTiC substrate concern as this can significantly affect the properties of the substrate.

Replacing carbon atoms with oxygen atoms in the TiC structure would significantly alter its properties. This affects the crystal structure as oxygen atom is larger than carbon and has a different electronic configuration. Substituting carbon atoms with oxygen atoms can cause distortions and strains in the surrounding crystal lattices. The mismatch in size might create vacancies in the lattices to accommodate the larger oxygen atoms.

Furthermore, oxygen forms ionic bonds with titanium, which the bonds are quite strong, but not as strong as the covalent network of carbon-titanium bonds in TiC. Ionic bonds involve the electrostatic attraction between oppositely charged ions. Even the ionic bonds are strong, but they generally lack the directional characteristic of covalent bonds. However, these bonds are not very flexible. As they are stressed, the ions cannot easily rearrange or slide past each other, leading to brittle fracture. The Mohs hardness of TiO_2 is about 5 to 6. Covalent bonds involve the sharing of electrons between atoms, often in specific directions determined by the atomic orbitals involved. This directionality creates a strong and rigid connection, resisting deformation more effectively. The titanium carbide features strong covalent bonds between titanium and carbon atoms. These directional bonds create a very rigid structure, making TiC exceptionally hard (Mohs hardness is about nine up to 9.5). Oxygen might not contribute to the ductility compared to carbon, potentially making the material more brittle and prone to cracking.

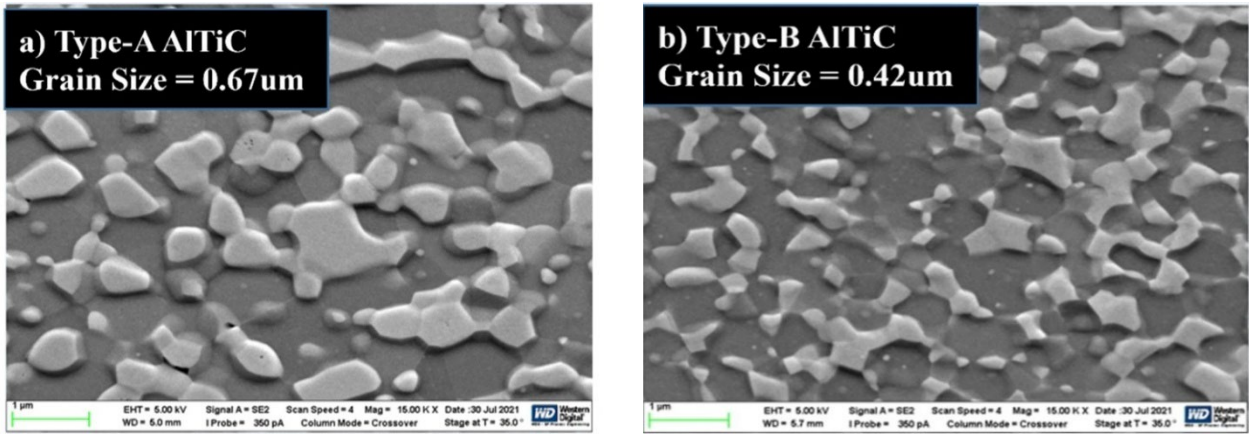

Figure 5. Scanning electron micrographs of (a) type-A AlTiC, and (b) type-B AlTiC substrates wafer.

Table 2. AlTiC substrate C/Ti ratio and chemical composition by EMPA.

Wafer Substrate	AlTiC Composition		
	Al_2O_3	TiC	$TiC_{1-x}O_x$
type-A AlTiC	51.90%	48.10%	0.0%
type-B AlTiC	52.20%	44.90%	2.9%

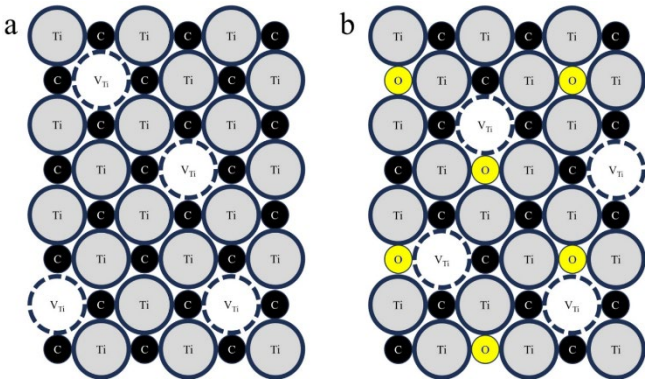

Figure 6. Rietveld modeling of TiC lattice structures of (a) type-A AlTiC and (b) type-B AlTiC substrate wafer.

Based on all the results, the type-B AlTiC substrate is a strong alternative for next-generation Hard Disk Drives (HDDs) because it offers better lapping and machining efficiency. Furthermore, these findings offer a key understanding of how AlTiC substrates affect the lapping friction and wear mechanisms (tribology). This knowledge will guide efforts to boost manufacturing productivity and achieve a better surface finish performance.

4. Conclusions

In this research, it was found that the lapping tribology is driven by the crystal structure and chemical bonding of the AlTiC substrates rather than the grain size. The type-B lower material removal rate resulting to rougher surface finish was mainly due weakening caused by the titanium oxycarbide phase, which was the dominant factor, outweighing the minimal contribution from grain-boundary strengthening (Hall-Petch effect). Furthermore, the grain size investigated in this study was between 420 nm to 670 nm, making it far too large for the inverse Hall–Petch effect which involves softening at exceedingly small grain sizes typically below 100 nm to be a relevant mechanism. The findings also highlight the importance of lapping parameters optimization to balance material removal rate (process productivity and efficiency) and surface finish (magnetic head reliability and areal density performance).

Acknowledgements

The authors would like to thank the Interdisciplinary program in Nanoscience and Technology, Graduate School, Chulalongkorn University and Western Digital Storage Technologies (Thailand) Ltd. for their supports.

References

[1] B. Liu, M. Zhang, S. Yu, L. Gonzaga, H.S. Hor, and J. Xu, "Femto slider: fabrication and evaluation," *IEEE Transactions on Magnetics,* vol. 39, no. 2, pp. 909-914, 2003.

[2] L. Cheng, Z. Xie, G. Liu, W. Liu, and W. Xue, "Densification and mechanical properties of TiC by SPS-effects of holding time, sintering temperature and pressure condition," *Journal of the European Ceramic Society*, vol. 32, no. 12, pp. 3399–3406, 2012.

[3] M. Herrmann, and J. Räthel, "Hot pressing and hot isostatic pressing," *Elsevier eBooks*, pp. 270–277, 2020

[4] H. H. Gatzen, J. C. Maetzig, and M. K. Schwabe, "Precision machining of rigid disk head sliders," *IEEE Transactions on Magnetics,* vol. 32, no. 3, pp. 1843–1849, 1996.

[5] H. H. Gatzen, and J. C. Maetzig: "Nanogrinding," *Precision Engineering-journal of The International Societies for Precision Engineering and Nanotechnology*, vol. 21, no. 2–3, pp. 134–139, 1997.

[6] D.-E. Kim, K.-H. Chung, and K.-H. Cha, "Tribological design methods for minimum surface damage of HDD slider," *Tribology International*, vol. 36, no. 4–6, pp. 467–473, 2003.

[7] H. H. Gatzen, X. Ma, M. Scherge, M. S. Jhon, and C. L. Bauer, "Observations regarding the tribological properties of SiC and AlTiC sliders," *IEEE Transactions on Magnetics,* vol. 32, no. 5, pp. 3783–3785, 1996.

[8] J. L. Sullivan, B. Shi, and S.O. Saied, "Microtribological studies of two-phase Al_2O_3–TiC ceramic at low contact pressure," *Tribology International,* vol. 38, no. 11–12, pp. 987–994, 2005.

[9] S. Jitphayomkun, P. Dechadilok, D. Tungasmita, S. Tungasmita, "Investigation on the tribological characteristics of lubricated Al_2O_3-TiC surface," *Journal of Metals, Materials and Minerals*, vol. 29, no. 1 pp. 63–68, 2019.

[10] H. Engqvist, and B. Uhrenius, "Determination of the average grain size of cemented carbides," *International Journal of Refractory Metals and Hard Materials*, vol. 21, no. 1–2, pp. 31–35, 2003

[11] D. Adamovic, and F. Zivic, "Hardness and non-destructive testing (NDT) of ceramic matrix composites (CMCs)," *Encyclopedia of Materials: Composites*, pp. 183–201, 2021.

[12] J. Gao, W. D. Luedtke, D. Gourdon, M. Ruths, J. N. Israelachvili, and U. Landman, "Frictional forces and Amontons' law: From the molecular to the macroscopic scale," *The Journal of Physical Chemistry B*, vol. 108, no. 11, pp. 3410–3425, 2004.

[13] T. Deaconescu, and A. Deaconescu, "Developing an analytical model and computing tool for optimizing lapping operations of flat objects made of alloyed steels," *Materials*, vol. 13, no. 6, pp. 1343–1343, 2020.

[14] K. F. Cai, D. S. McLachlan, N. Axen, and R. Manyatsa, "Preparation, microstructures and properties of Al_2O_3–TiC composites," *Ceramics International*, vol. 28, no. 2, pp. 217–222, 2002.

[15] M. Madhan, and G. Prabhakaran, "Microwave versus conventional sintering: Microstructure and mechanical properties of Al_2O_3–SiC ceramic composites," *Boletín de la Sociedad Española de Cerámica y Vidrio*, vol. 58, no. 1, pp. 14–22, 2018.

[16] Z. Yin, C. Huang, B. Zou, H. Liu, H. Zhu, and J. Wang, "Study of the mechanical properties, strengthening and toughening mechanisms of Al_2O_3/TiC micro-nano-composite ceramic tool material," *Materials Science and Engineering: A*, vol. 577, pp. 9–15, 2013.

[17] Z. Cordero, B. E. Knight, and C. A. Schuh, "Six decades of the Hall–Petch effect – a survey of grain-size strengthening studies on pure metals," *International Materials Reviews*, vol. 61, no. 8, pp. 495–512, 2016.

[18] M. A. Meyers, A. Mishra, and D. J. Benson, "Mechanical properties of nanocrystalline materials," *Progress in Materials Science*, vol. 51, no. 4, pp. 427–556, 2006.

[19] J. Schiøtz, F. D. Di Tolla, and K. W. Jacobsen, "Softening of nanocrystalline metals at very small grain sizes," *Nature,* vol. 391, pp. 561–563, 1998.

[20] S. Z. Chavoshi, and S. Xu, "Tension-compression asymmetry in plasticity of Nano twinned 3C-SiC nanocrystals," *Journal of Applied Physics*, vol. 124, no. 9, 2018.

[21] Q. An, and W. A. Goddard, "Nanotwins soften boron-rich boron carbide ($B_{13}C_2$)," *Applied Physics Letters*, vol. 110, no. 11, 2017

[22] S. Z. Chavoshi, and S. Xu, "Twinning effects in the single/nanocrystalline cubic silicon carbide subjected to nano-indentation loading," *Materialia*, vol. 3, pp. 304–325, 2018

[23] M. Ivanovskaya, E. Ovodok, D. Kotsikau, I. Azarko, M. Micusik, M. Omastova, and V. Golovanov, "Structural transformation and nature of defects in titanium carbide treated in different redox atmospheres," *RSC Advances*, vol. 10, no. 43, pp. 25602–25608, 2020.